WILEY-VCH

Dual Excitation Transient Photocurrent Measurement for Charge Transfer Studies in Nanocarbon Hybrids and Composites

Alexey S. Cherevan and Dominik Eder**

Dr. A. S. Cherevan, Prof. Dr. D. Eder

Institute of Materials Chemistry,
Technische Universität Wien
Getreidemarkt 9/BC/02/A34
1060, Vienna, Austria

alexey.cherevan@tuwien.ac.at
dominik.eder@tuwien.ac.at

Keywords: hybrids, composites, nanocarbons, interfacial charge transfer, transient photocurrent

Abstract

A new technique, dual excitation transient photocurrent measurement (DETPM), which enables to deconvolute intrinsic photoresponse of nanocarbons from interfacial charge transfer processes in nanocarbon-inorganic hybrids and composites, is reported. The technique can be extended to other nanocarbon-based systems with a wide range of semiconductors and allows quantitative analysis of the charge transfer process.

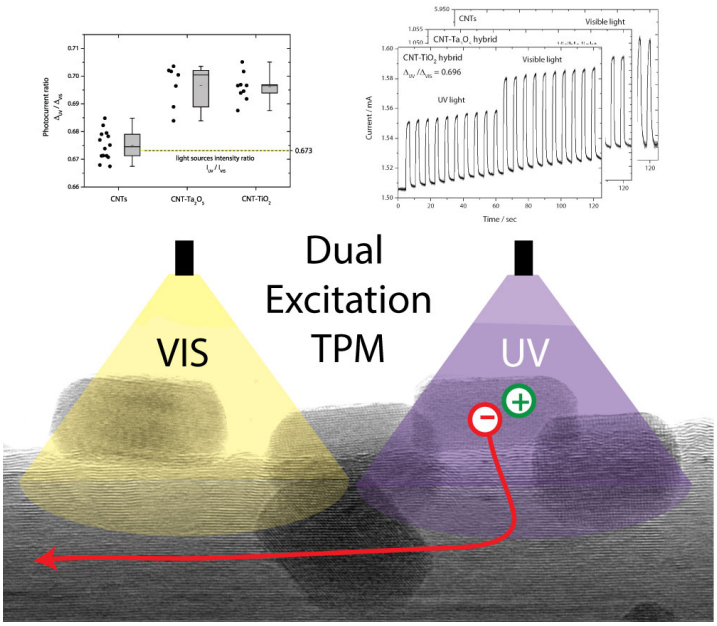

Nanocarbon-inorganic hybrids – where a functional compound is deposited onto a nanocarbon in a form of nanoparticles, layers or thin films – constitute a novel class of materials that have already demonstrated their potential in various light-to-fuel and light-to-electricity conversion applications such as photocatalysis.[1–3] Benefits of the hybrids arise from the strong ability of the nanocarbons to withdraw,[4,5] store[6] and conduct[7–9] photoexited electrons from the photocatalyst as depicted in **Figure 1a**. Such a charge transfer process leads to efficient spatial separation of the electrons from the holes, slows down recombination rates, and thus often results in a better photocatalytic performance of the hybrids as more charges are available for subsequent redox reactions. This key process, however, is rather difficult to record and assess and only a limited number of techniques have been applied to obtain information on interfacial charge transfer in nanocarbon hybrids.

Photoluminescence (PL) has been used to monitor PL quenching, which has been attributed to either transfer of photoexcited charges or energy transfer between semiconductor to nanocarbon.[10–13] For example, *Kamat et al.* have added increasing concentrations of both carbon nanotubes (CNTs)[14] and graphene[15] to ZnO nanoparticle solution and observed a decrease in PL signal, from which they deduced the presence of electron transfer from ZnO to the nanocarbon. However, such a loss of PL signal could also originate, for example, from additional light absorption due to the gradually increasing fraction of the nanocarbon as well as contributions arising from particle size and shape differences. In addition to that, PL is only applicable to a limited number of compounds, i.e. fluorescent materials.

Transient photocurrent measurements (TPM) constitute an alternative method, in which chronoamperometry data (current vs time) of a solid sample are recorded under an external bias upon illumination with light. The method relies on the fact that when the photoexcited charges are transferred into the nanocarbon, additional carriers completing the electric circuit are created therefore resulting in a so-called additional photocurrent. TPM has already been applied to nanocarbon hybrids and composites;[6,16–22] however, none of these works have considered that this photoresponse could also originate from the nanocarbon itself. In fact, it is known that the electrical properties of CNTs[23,24] and graphenes[25] are strongly influenced by light, hence this inherent behavior of the nanocarbons need to be considered for TPM on nanocarbon-based hybrids and composites.

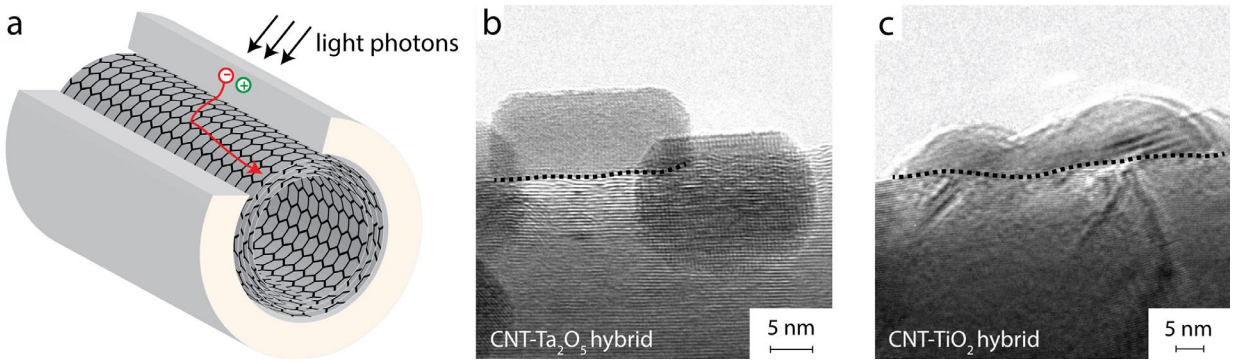

Figure 1. (a) Illustration of a nanocarbon-inorganic hybrid and the charge transfer of the photoexcited charges from the semiconductor to the nanocarbon; and TEM images of the (b) CNTs-Ta_2O_5 and (c) CNTs-TiO_2 hybrids. The dashed lines highlight the tight and extended interface between the nanocarbon and the oxide layers.

The photoresponse of CNTs has generated considerable debate during last decades and only recently its bolometric nature has been experimentally confirmed.[26] The theory implies that light illumination of CNTs creates excitons with unusually high binding energies,[27] which cannot directly contribute to the photoconductivity. In this scenario, they have to dissociate thermally therefore locally heating up the nanocarbon matrix. The increase in temperature leads to an increase in conductivity of the CNTs (in contrast to 3D metals, as explained by the Luttinger liquid model for one-dimensional conductors[28,29]) and results in additional photocurrent.

This knowledge, however, has not yet been implemented into practice and standard photocurrent measurements on nanocarbon hybrids and composites are still conducted without considering the photoresponse of bare CNTs. Here we report a new technique, which we describe as dual excitation transient photocurrent measurement (DETPM). This technique allows for distinguishing the bolometric effect (i.e. intrinsic conductivity change due to heat produced by light irradiation) from a potential photoexcited charge transfer in CNTs-based hybrids. We have tested this technique on two high-performance hybrids, CNT-TiO_2 and CNT-Ta_2O_5, and explicitly demonstrate the presence of the charge transfer from the semiconductor to the nanocarbon in both cases.

We synthesized the CNT-Ta_2O_5 hybrid via a modified sol-gel process and the CNT-TiO_2 hybrid via atomic layer deposition process (details on synthesis in Experimental Section and characterization in ESI). We aimed to create hybrids with a high degree of conformal coating and an extended interface between the CNTs and the metal oxide to maximize the interfacial charge transfer. SEM images of both hybrids in Figure S1 confirm the presence of uniform coating on the nanocarbon surface and demonstrate homogeneity of the samples. As further

revealed by HRTEM in Figure 1b and c a tight interface between the two components was established in both cases. Importantly, all samples used for the TPM were prepared in a form of free-standing macroscopic membranes to eliminate any substrate contribution. In a typical DETPM experiment, a macroscopic membrane, containing either pure CNTs (i.e. reference) or the CNT-based hybrids, was connected to two electrodes as shown in **Figure 2a** and a small bias was applied to establish a constant current.

In order to distinguish between the potential charge transfer and the bolometric effect in our hybrid samples we relied on the fact that the intrinsic photoresponse of CNTs is directly proportional to light intensity, but not dependent on its wavelength (due to its bolometric nature);[26] in contrast, photoexcitation in semiconducting oxides only occurs when the photon energy is larger than the oxide band gap (i.e. wavelength dependency). In the present work, we chose hybrids with Ta_2O_5 and TiO_2, both of which require light irradiation below 400 nm for photoexcitation due to their large band gap energies of 3.8 and ca. 3.1 eV, respectively (Figure 2b).

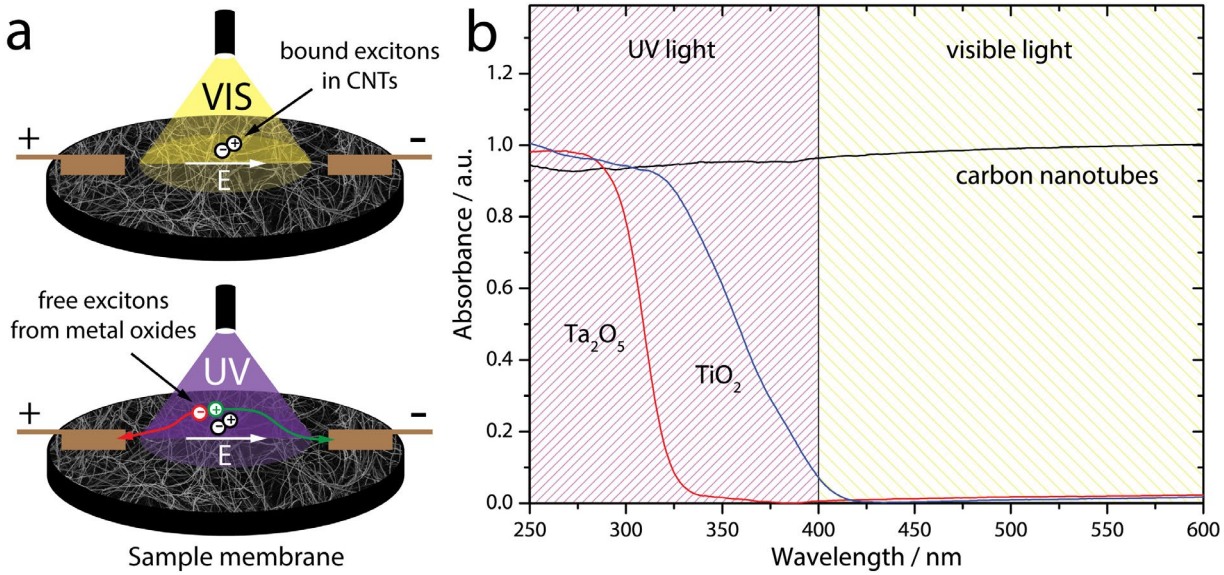

Figure 2. (a) Schemes of the DETPM experiment performed under visible and UV light illumination: black e-h pair represents bound excitons responsible for the intrinsic photoresponse of the CNTs; red-green e-h pair represents free-moving excitons that can be produced in the metal oxides only upon absorption of the UV light photon. (b) Diffuse reflectance spectra of CNTs as well as Ta_2O_5 and TiO_2 chosen for hybridization: patterned areas indicate operating wavelength ranges of the UV and visible light sources used in DETPM.

The key feature of DETPM was to use two light sources (i.e. "dual excitation") that operate in different wavelength regimes (Figure 2): one in the visible range (above 400 nm) that only stimulates the intrinsic (i.e. bolometric) photoresponse of CNTs, and a second in the UV

range (below 400 nm) that additionally activates the semiconductor and induces a photoresponse via interfacial charge transfer. More details including technical information about the light sources are summarized in **Table 1** and Experimental Section.

Table 1. Characteristics of the light sources used to perform DETPM.

Light source	Operating wavelength range / nm	Total power output / W	Power ratio I_{UV}/I_{VIS}
UV	240-400	1.77	0.673
visible	400-600	2.63	

In a typical experiment, a sample was illuminated with short light-on pulses (e.g. 2 s) to avoid overheating and the chronoamperometry data were recorded with time intervals of 3 ms. To allow statistical evaluation, at least 10 light on/off illumination cycles (UV and visible) were applied in each experiment. Furthermore, to eliminate any influence imposed by the sample preparation conditions (e.g. different mass of the CNTs and the oxides, number of tube-tube contact points, interface area to the electrodes, etc.) on the extent of the resulting photocurrent, we measured the difference in currents between dark and illumination (Δ) and characterized each of the samples with an internal ratio of the photocurrent increase under UV and visible light irradiation Δ_{UV}/Δ_{VIS} (details in Experimental Section and Figure 3b):

$$\frac{\Delta_{UV}}{\Delta_{VIS}} = \frac{i^{t}_{UV} - i^{0}_{UV}}{i^{t}_{VIS} - i^{0}_{VIS}}$$

We first investigated the pure CNTs samples during short light on-off cycles using both UV and visible light sources. **Figure 3a** confirms that pure CNT membranes exhibit a photocurrent response under light illumination. As expected, the measured current increased rapidly under light-on condition and decreased when the light was switched off. Our experiments also show that the photocurrent increase rate reaches its maximum within the first 150 ms of light illumination cycle (see analysis of derivatives in ESI, Figure S5 and Table S1). This result is in line with the characteristic response times of the bolometric effect reported for CNTs.[26]

The DETPM data were assessed statistically to derive Δ_{UV}/Δ_{VIS} ratio of the photocurrent increase for each of the samples (Table S2). Importantly, the photoresponse of the CNT sample is stronger under visible light compared to UV light, however, the calculated ratio between the photocurrents (Δ_{UV}/Δ_{VIS} = 0.675, Figure 3b) almost exactly matches the ratio of power outputs of both light sources (I_{UV}/I_{VIS} = 0.673, Table 1). This further supports the

hypothesis that the observed photoresponse in the pure CNT membranes has a bolometric nature.

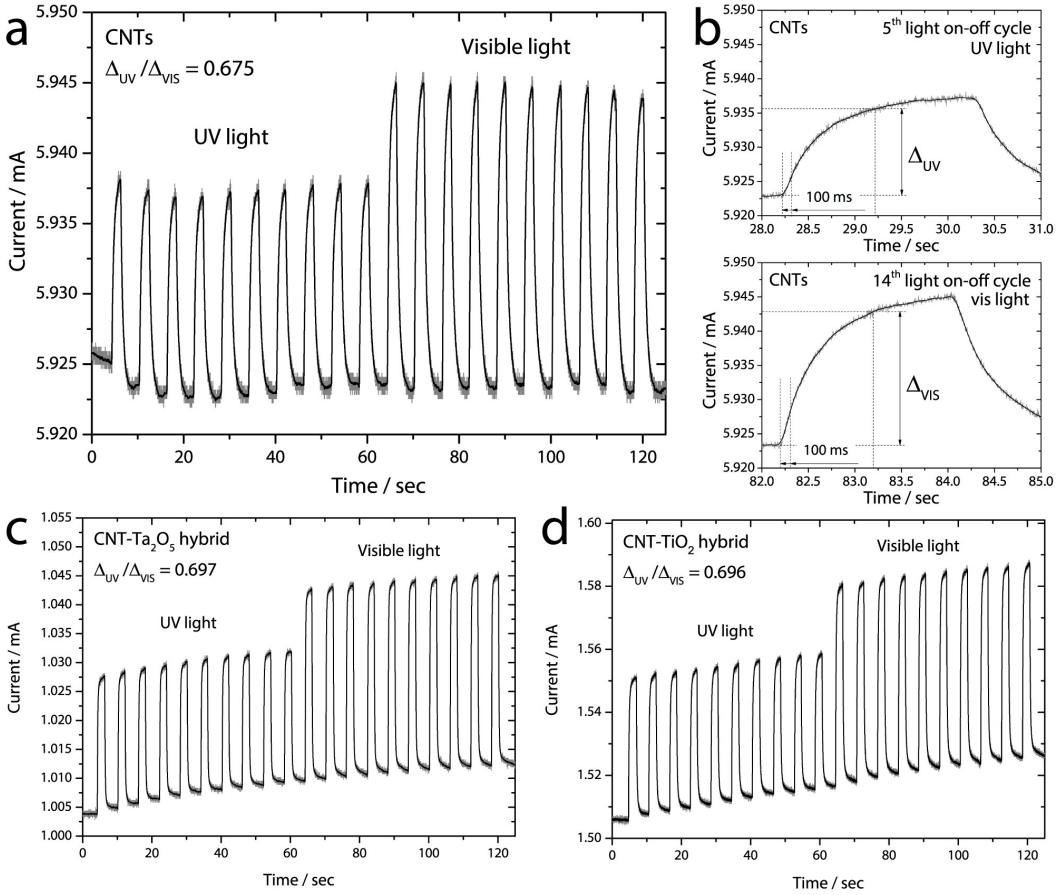

Figure 3. Transient photocurrent response obtained for (a) pure CNTs (d) CNT-Ta_2O_5 and (e) CNT-TiO_2 sample under 2 s light on-off cycles of UV (10 cycles) and visible (10 cycles) light illumination and (b) magnified regions of (a) showing exemplary light on-off cycles performed under UV (top) light and visible light (bottom). Photocurrent increase after 1 s of light illumination (Δ_{UV} and Δ_{VIS}) was calculated for each light on-off cycle.

The photoresponse of the CNT-TiO_2 and CNT-Ta_2O_5 hybrids towards both light sources at first appears similar to the pure CNTs (Figure 3c and d). However, a statistical evaluation of the data revealed a comparably larger photocurrent under UV irradiation, thus yielding significantly higher Δ_{UV}/Δ_{VIS} ratios (0.696 and 0.697, respectively as shown **Figure 4**). This confirms the presence of an additional contribution to the photocurrent under UV illumination in both hybrids. A contribution through thermoelectric response can be ruled out due to the symmetrical design of our device (Figure 2a). Furthermore, the nature of our method, which is based on calculating relative Δ_{UV}/Δ_{VIS} ratios, renders contributions of sample geometry, structure and morphology negligible. Therefore, we can directly assign the increased Δ_{UV}/Δ_{VIS} ratio to charge transfer of the photoexcited electrons between semiconductor and CNT.

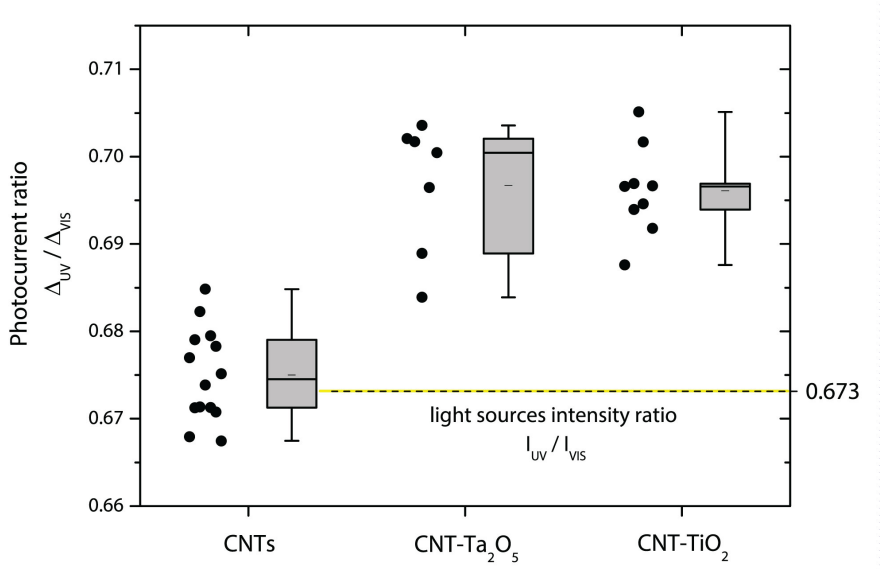

Figure 4. Statistical evaluation (including error bars) of the Δ_{UV}/Δ_{VIS} ratio of the photocurrent increases after 1 s of light illumination for CNTs-Ta_2O_5 and CNTs-TiO_2 nanocarbon hybrids along with the pure CNTs reference. Ratio of the intensity outputs of UV and visible light sources (I_{UV}/I_{VIS}=0.673) is highlighted with a dashed line.

In conclusion, we developed a new technique, the dual excitation transient photocurrent measurement (DETPM), which enables to deconvolute intrinsic effects of nanocarbons (e.g. based on the bolometric response) from charge transfer processes in nanocarbon-inorganic hybrids and composites by taking advantage of the different wavelength dependency of these two processes. We have successfully applied this method to two model hybrids CNTs-Ta_2O_5 and CNTs-TiO_2 and have been able to confirm directly the presence of a charge transfer in both systems. DETPM is a simple and straightforward technique that can be used to characterize samples independently on their geometry and preparation method. It can be easily extended to other nanocarbon-based systems with a wide range of semiconductors (e.g. by using suitable light sources and optical filters). Furthermore, it allows quantitative analysis of the charge transfer process and thus its direct correlation with the hybrid's performance in applications, where charge separation is required, including photocatalysis, photovoltaics, electrochemical sensing, electrocatalysis and energy storage.

Experimental Section

Synthesis of CNTs:

CNTs were grown via a continuous-flow chemical vapour deposition technique using ferrocene as the catalyst precursor and toluene as carbon feed. The reaction temperature was kept at 760 °C and Ar was used as the carrier gas (flow 400 mL/min). In a typical experiment, 22 mL of 4 wt. % ferrocene in toluene solution was injected into the reactor at a rate of 5.4 mL/h for 0.5 h. As grown CNTs were further purified in argon at 1000 °C to remove amorphous carbon and, partially, other impurities.

Synthesis of model hybrids:

CNT-Ta_2O_5 hybrids were synthesized via a modified sol-gel process[30] to form a macroscopic sample where CNT-CNT contacts will be maintained. First, CNTs (8.9 mg) were dispersed within 30 ml of EtOH solution via ultrasound treatment and shaped into a membrane using vacuum filtration. The sample was then placed into an autoclave that contained 10 microL of benzyl alcohol and treated at 150 °C for 2 hours to non-covalently modify the intrinsically hydrophobic nanocarbon surface with OH groups required to provide strong interaction with polar Ta precursor molecules.[31] The filter cake was further placed into a petri dish that contained absolute EtOH (20 ml), while $Ta(OEt)_5$ solution (99 mg dissolved in 20 ml of absolute EtOH) was dropwise added under slow stirring thus ensuring controlled deposition of Ta_2O_5 layer onto the CNT surface. The dried sample was then calcined at 800 °C for 1 h using Ar atmosphere to crystallise the oxide layer. The final CNT-Ta_2O_5 hybrid product (10.6 mg) was used for the photocurrent measurements. Mass fraction of CNTs in the sample is 84 % as calculated from the membrane mass increase after Ta_2O_5 deposition.

CNT-TiO_2 hybrids were prepared via atomic layer deposition process. Similarly, CNTs (10 mg) were first shaped into a membrane using vacuum filtration. The sample was non-covalently modified with pyrenecarboxylic acid by subjecting the sample to the autoclaving at 215 °C for 2 h with 1 ml 1 mg/ml PCA in EtOH solution.[32] 200 ALD deposition cycles were accomplished at 150 °C using $Ti(N(CH_3)_2)_4$ (pre-heated to 75 °C) and H_2O. The resulting CNTs-TiO_2 hybrid was further subjected to annealing at 500 °C for 1 h using Ar atmosphere to crystallise the oxide layer yielding 17.2 mg of the product. Mass fraction of CNTs in the sample is 58 % as calculated from the membrane mass increase after TiO_2 deposition. The final product was used for the photocurrent measurements.

CNT membranes were prepared similarly by using vacuum filtration of the CNT dispersion in EtOH and were used here as a reference to show the presence of the intrinsic photocurrent as a result of the bolometric effect.

Characterisation methods

SEM images were acquired using Zeiss XB 1540 EsB scanning electron microscope. Typically acceleration voltage of 2 keV and secondary electron detection mode were used. TEM images were obtained using FEI Tecnai F20 transmission electron microscope equipped with a field emission gun in bright field mode using 200 keV acceleration voltage. The sample was prepared from a suspension in ethanol without ultrasonication, using a copper Lacey carbon coated grids (Plano, 200 mesh). XRD was performed using Bruker D8 Advance machine with Bragg-Brentano geometry equipped with a Ni filter and a Lynxeye super speed detector using a Cu Kα irradiation with λ_1 of 1.540596 Å and λ_2 of 1.544410 Å with the ratio of 0.442227. XPS was performed using ESCALAB 250 from Thermo VG Scientific with monochromatic Al K_α X-rays. Quantitative information about the surface composition was calculated from survey spectra using the standard Scofield sensitivity factors. Raman spectroscopy data were acquired with Jobin Yuon Horiba LABRAM HR equipped with a Ne:YAG-Laser (lambda = 532 nm).

Photocurrent measurements

Lumatec deep UV light source (200 W super pressure Hg lamp) was used to illuminate the samples with the light in the wavelength range of 240-400 nm (UV light regime) and of 400-600 nm (visible light regime). The light was delivered to the sample membrane by means of an optical fibre (Lumatec, series 250, 1 m long, 5 mm in diameter). Light intensity was controlled by using the power energy meter (Thorlabs, PM100D).

Dual excitation transient photocurrent measurement (DETPM) was further employed to compare photoresponse of the pure CNTs and both hybrids under both UV and visible light illumination. In a single experiment, a sample membrane (CNTs, CNT-Ta_2O_5 or CNT-TiO_2) was connected to two electrodes as shown in Figure 2a, while a small bias (0.01 V) was applied to establish a constant current. The measured current was typically in the range of 10^{-3} A. Each sample membrane was illuminated with 2 sec light-on pulses followed by 4 sec of light-off regime to allow thermal relaxation of the sample in two different wavelengths ranges: UV light mode where both mechanisms of photocurrent increase are activated and white light mode which is only capable of promoting the bolometric response (no possible photoexcitation in the semiconducting oxides). To allow statistical evaluation, at least 10 light

on/off illumination cycles were applied in each experiment. Besides, to eliminate issues related to morphology of the different sample membranes (e.g. mass of the CNTs and the resulting hybrid, number of tube-tube contact points, interface area to the electrodes), every sample (of both hybrids and pure CNTs) was examined be means of both light sources to extract photocurrent increase under light compared to dark conditions (because the geometry of the sample membrane is unchanged during the experiment, the measured photocurrent increase Δ can be directly related to the increased number of charge carriers or conductivity of the matrix). We further calculated an internal value of the ratio between the photocurrent increases caused by the UV and visible light sources Δ_{UV}/Δ_{VIS}, while this ratio is characteristic for the properties of the material. I (t) data were recorded with time intervals of 3 ms by means of a photoelectrochemical workstation (Metrohm) controlled with Nova software.

Supporting Information

Supporting Information is available from the Wiley Online Library or from the author and contains information on synthesis and characterization (SEM, XRD, Raman, XPS) of CNT and the CNT-based hybrids. It further contains detailed description of the DETPM procedure as well as the derivative analysis and statistical photocurrent data evaluation. Refer to this link.

Acknowledgements

We would like to acknowledge D. Dieterle for XRD measurements, P. Gebhardt for TEM studies, N. Kemnade for ALD synthesis, J. Wang for Raman measurements, T. Reuter for XPS studies and C. J. Shearer for the help with electrochemistry experiments. We would also like to thank G. Wilde, H.-D. Wiemhöfer and J.J. Vilatela for discussions. The research leading to these results has received funding from the European Union Seventh Framework Programme under the grant agreement № 310184, CARINHYPH project.

References

[1] D. Eder, *Chem. Rev.* **2010**, *110*, 1348.
[2] C. J. Shearer, A. Cherevan, D. Eder, *Adv. Mater.* **2014**, *26*, 2295.
[3] S. Cao, J. Yu, *J. Photochem. Photobiol. C Photochem. Rev.* **n.d.**, DOI 10.1016/j.jphotochemrev.2016.04.002.
[4] Z. Mou, S. Yin, M. Zhu, Y. Du, X. Wang, P. Yang, J. Zheng, C. Lu, *Phys. Chem. Chem. Phys.* **2013**, *15*, 2793.
[5] T. Peng, K. Li, P. Zeng, Q. Zhang, X. Zhang, *J. Phys. Chem. C* **2012**, *116*, 22720.
[6] H. Kim, G. Moon, D. Monllor-Satoca, Y. Park, W. Choi, *J. Phys. Chem. C* **2012**, *116*, 1535.
[7] F. Pei, Y. Liu, S. Xu, J. Lü, C. Wang, S. Cao, *Int. J. Hydrog. Energy* **2013**, *38*, 2670.
[8] J. Zhou, G. Tian, Y. Chen, X. Meng, Y. Shi, X. Cao, K. Pan, H. Fu, *Chem. Commun.* **2013**, *49*, 2237.
[9] X.-J. Lv, W.-F. Fu, H.-X. Chang, H. Zhang, J.-S. Cheng, G.-J. Zhang, Y. Song, C.-Y. Hu, J.-H. Li, *J. Mater. Chem.* **2011**, *22*, 1539.

[10] L. Ge, C. Han, *Appl. Catal. B Environ.* **2012**, *117–118*, 268.
[11] A. Suryawanshi, P. Dhanasekaran, D. Mhamane, S. Kelkar, S. Patil, N. Gupta, S. Ogale, *Int. J. Hydrog. Energy* **2012**, *37*, 9584.
[12] Q. Xiang, J. Yu, M. Jaroniec, *J. Phys. Chem. C* **2011**, *115*, 7355.
[13] I. V. Lightcap, P. V. Kamat, *J. Am. Chem. Soc.* **2012**, *134*, 7109.
[14] F. Vietmeyer, B. Seger, P. V. Kamat, *Adv. Mater.* **2007**, *19*, 2935.
[15] G. Williams, P. V. Kamat, *Langmuir* **2009**, *25*, 13869.
[16] I. Robel, B. A. Bunker, P. V. Kamat, *Adv. Mater.* **2005**, *17*, 2458.
[17] J. Yu, T. Ma, S. Liu, *Phys. Chem. Chem. Phys.* **2011**, *13*, 3491.
[18] L. Jia, D.-H. Wang, Y.-X. Huang, A.-W. Xu, H.-Q. Yu, *J. Phys. Chem. C* **2011**, *115*, 11466.
[19] P. D. Tran, S. K. Batabyal, S. S. Pramana, J. Barber, L. H. Wong, S. C. J. Loo, *Nanoscale* **2012**, *4*, 3875.
[20] A. Ye, W. Fan, Q. Zhang, W. Deng, Y. Wang, *Catal. Sci. Technol.* **2012**, *2*, 969.
[21] L. Ge, C. Han, *Appl. Catal. B Environ.* **2012**, *117–118*, 268.
[22] C. Han, Z. Chen, N. Zhang, J. C. Colmenares, Y.-J. Xu, *Adv. Funct. Mater.* **2015**, *25*, 221.
[23] R. Lu, J. J. Shi, F. J. Baca, J. Z. Wu, *J. Appl. Phys.* **2010**, *108*, 084305.
[24] P. Stokes, L. Liu, J. Zou, L. Zhai, Q. Huo, S. I. Khondaker, *Appl. Phys. Lett.* **2009**, *94*, 042110.
[25] F. Xia, T. Mueller, Y.-M. Lin, A. Valdes-Garcia, P. Avouris, *Nat. Nanotechnol.* **2009**, *4*, 839.
[26] M. E. Itkis, F. Borondics, A. Yu, R. C. Haddon, *Science* **2006**, *312*, 413.
[27] A. Jorio, G. Dresselhaus, M. S. Dresselhaus, *Carbon Nanotubes: Advanced Topics in the Synthesis, Structure, Properties and Applications*, Springer Science & Business Media, **2007**.
[28] J. M. Luttinger, *J. Math. Phys.* **1963**, *4*, 1154.
[29] E. Graugnard, P. J. de Pablo, B. Walsh, A. W. Ghosh, S. Datta, R. Reifenberger, *Phys. Rev. B* **2001**, *64*, 125407.
[30] A. S. Cherevan, P. Gebhardt, C. J. Shearer, M. Matsukawa, K. Domen, D. Eder, *Energy Environ. Sci.* **2014**, *7*, 791.
[31] D. J. Cooke, D. Eder, J. A. Elliott, *J. Phys. Chem. C* **2010**, *114*, 2462.
[32] N. Kemnade, C. J. Shearer, D. J. Dieterle, A. S. Cherevan, P. Gebhardt, G. Wilde, D. Eder, *Nanoscale* **2015**, *7*, 3028.